A&A 444, 643–649 (2005)
DOI: 10.1051/0004-6361:20053098
© ESO 2005

Astronomy & Astrophysics

Candidate spectroscopic binaries in the Sloan Digital Sky Survey⋆

D. Pourbaix[1,2,⋆⋆], G. R. Knapp[1], P. Szkody[3], Ž. Ivezić[3], S. J. Kleinman[4], D. Long[4], S. A. Snedden[4], A. Nitta[4], M. Harvanek[4], J. Krzesinski[4,5], H. J. Brewington[4], J. C. Barentine[4], E. H. Neilsen[6], and J. Brinkmann[4]

[1] Department of Astrophysical Sciences, Princeton University, Princeton, NJ 08544-1001, USA
e-mail: [pourbaix;gk]@astro.princeton.edu
[2] Institut d'Astronomie et d'Astrophysique, Université Libre de Bruxelles, CP. 226, Boulevard du Triomphe, 1050 Bruxelles, Belgium
e-mail: pourbaix@astro.ulb.ac.be
[3] Department of Astronomy, University of Washington, Box 351580, Seattle, WA 98195, USA
e-mail: [szkody;ivezic]@astro.washington.edu
[4] Apache Point Observatory, PO Box 59, Sunspot, NM 88349, USA
e-mail: [sjnk;long;snedden;ank;harvanek;jurek;hbrewington;jcb;jb]@apo.nmsu.edu
[5] Mt. Suhora Observatory, Cracow Pedagogical University, ul. Podchorazych 2, 30-084 Cracow, Poland
[6] Fermi National Accelerator Laboratory, PO Box 500, Batavia, IL 60510, USA
e-mail: neilsen@fnal.gov

Received 21 March 2005 / Accepted 21 August 2005

ABSTRACT

We have examined the radial velocity data for stars spectroscopically observed by the Sloan Digital Sky Survey (SDSS) more than once to investigate the incidence of spectroscopic binaries, and to evaluate the accuracy of the SDSS stellar radial velocities. We find agreement between the fraction of stars with significant velocity variations and the expected fraction of binary stars in the halo and thick disk populations. The observations produce a list of 675 possible new spectroscopic binary stars and orbits for eight of them.

Key words. instrumentation: spectrographs – stars: binaries: spectroscopic

1. Introduction

This paper is based on an investigation of the radial velocity accuracy obtainable for stars observed in the Sloan Digital Sky Survey (SDSS) which we carried out in support of current and upcoming observations of Galactic stellar kinematics using SDSS spectroscopy (Beers et al. 2004). In the course of this investigation, we were able to identify a large number of confirmed and candidate binary stars. While SDSS data have been used in several recent studies of binary stars, in particular of dwarf M-white dwarf pairs and cataclysmic variables (Szkody et al. 2002, 2003a,b, 2004, 2005; Raymond et al. 2003; Pourbaix et al. 2004a; Smolčić et al. 2004), this represents the first detection of spectroscopic binaries in SDSS. This paper presents both of these results. The SDSS data are described in Sects. 2 and 3, and in Sect. 4 we compare velocities observed at different epochs and examine their precision. Almost all of the stars with repeat observations have been observed only twice, and we analyze the distribution of velocity differences to derive the binary fraction. In a small number of cases (19) there are sufficient observations that a spectroscopic orbit can be derived, but only eight of these orbits prove to be robust. These objects are discussed in Sect. 5, where the full list of possible binary stars is also described.

2. The Sloan Digital Sky Survey

The Sloan Digital Sky Survey (SDSS) is a 5-band photometric survey of about 10 000 square degrees of the Northern sky to a depth of about 22.5 (r magnitude, point source) and a concurrent redshift survey of up to a million galaxies and 100 000 quasars selected from the imaging survey (York et al. 2000). The primary science goals of the project are to provide the data to investigate the large scale structure of the Universe and other extragalactic science. The photometric data are acquired almost simultaneously in five bands, u, g, r, i, and z, centered at approximate effective wavelengths of 3551, 4686, 6166, 7480 and 8932 Å (Fukugita et al. 1996) using a large-format CCD camera (Gunn et al. 1998) mounted on a dedicated 2.5 m telescope at the Apache Point Observatory (APO)

⋆ Table 4 is only available in electronic form at the CDS via anonymous ftp to cdsarc.u-strasbg.fr(130.79.128.5) or via http://cdsweb.u-strasbg.fr/cgi-bin/qcat?J/A+A/444/643
⋆⋆ Research Associate, F.N.R.S., Belgium.

Article published by EDP Sciences and available at http://www.edpsciences.org/aa or http://dx.doi.org/10.1051/0004-6361:20053098

in New Mexico. The imaging data are automatically reduced through a series of software pipelines which find and measure objects and provide photometric and astrometric calibrations to produce a catalogue of objects with calibrated magnitudes, positions and structure information (Lupton et al. 2001, 2003; Pier et al. 2003; Ivezić et al. 2004). The instrumental fluxes are calibrated via a network of primary and secondary stellar flux standards to AB_ν magnitudes (Oke & Gunn 1983; Fukugita et al. 1996; Hogg et al. 2001; Smith et al. 2002) which are accurate to about 1% in g, r, and i, 3% in u and 2% in z for bright (<20 mag) point sources. The bright magnitude limit is about 14. Absolute positions are accurate to about 50 mas in each coordinate (Pier et al. 2003).

Targets for spectroscopy are selected from the imaging data on the basis of their photometric properties. As well as the primary SDSS targets, stars in many different locations of color–magnitude space are selected to serve as spectrophotometric standards and to provide backup targets in regions of low galaxy density. The target objects are mapped (Blanton et al. 2003) onto aluminum 3° diameter fiber plug plates which feed the spectrographs. The pair of dual fiber-fed spectrographs (Uomoto et al. 1999) can observe 640 spectra at one time with a wavelength coverage of 3800–9200 Å and a resolution of 1800 to 2100. The fibers subtend an aperture of 3″ on the sky. The spectroscopic observations usually consist of three fifteen-minute exposures per spectroscopic plate.

The data are optimally extracted from the CCD images, flat-fielded and wavelength calibrated using arc spectra and the night-sky lines observed on the plate. A mean sky spectrum is subtracted from each object spectrum, which is then flux-calibrated with respect to the F star calibration spectra. Regions of the spectrum with bad data (for example, in the immediate wavelength vicinity of strong night sky lines) are flagged so that they will not be used in subsequent analysis. The resulting calibrated 1D spectra are fit to a series of templates of galaxies, quasars and stars to derive the spectral classification, redshift and redshift error of each object (D. Schlegel, in preparation).

There are several extensive libraries of stellar spectra, which can be used as templates for spectral type and radial velocity fitting. Our work began with the flux-calibrated spectra from the Elodie library (Prugniel & Soubiran 2001; Moultaka et al. 2004). However, since the Elodie spectra do not have as large wavelength coverage as do the SDSS spectra, they are not ideal for direct use as templates. The stellar templates were therefore used as follows. First, the Elodie spectra were matched against the SDSS spectra and used to extract spectra with a good signal-to-noise ratio (>15 per spectral resolution element), to assign best-fit spectral types and to correct the SDSS spectrum to a velocity of 0 $\mathrm{km\,s^{-1}}$ (the Elodie spectral library has systematic errors less than 1 $\mathrm{km\,s^{-1}}$). Next, the calibrated and typed SDSS spectra were used to select representative spectra of all observed spectral types. These spectra were used to construct templates by combining individual spectra and defining the principle components (see Heyer & Schloerb 1997) to produce a set of templates simulating a wide range of effective temperature, gravity and metallicity. These templates were then fit to all SDSS spectra directly in flux density-wavelength space, using χ^2 minimization to assign the most likely spectral type and redshift. For the subset of objects classified as stars, the assigned spectral type of each star is that of the best fit stellar template, and the radial velocity is calculated from the redshift necessary to bring the template spectrum and object spectrum into optimum alignment in wavelength space.

This process produces both a radial velocity and a radial velocity error for the best fit template, but there is a second source of radial velocity error, that arising from template mismatch. To evaluate this error, each SDSS stellar spectrum is fit to all 900 Elodie spectra and the standard deviation of the radial velocities of the 12 best-fit templates computed. This quantity can sometimes be much larger than the random error if there is significant template mismatch, and it is included in the total radial velocity error.

For the particular application discussed here, the investigation of radial velocity changes for a given star which are larger than the random errors and therefore may be due to binary motion, the errors introduced by template mismatch are less important, since the same template will be fitted to the stellar spectrum for each epoch of observation (except in very rare cases, such as that shown in Fig. 6 below), and indeed this was checked for the multiply-observed stars analyzed in the next sections. Some stars, however, may have no good template available because their lines are broadened by rapid rotation, and the velocity errors will not be well determined. Fortunately, such stars are very seldom found in the SDSS data base.

The SDSS data are described in the data release papers by Abazajian et al. (2003, 2004, 2005) and documented at the web sites listed therein and at `http://www.sdss.org`, where the sky coverage of the SDSS observations is also described.

3. Multiple radial velocity observations

The objects which were both targeted and spectroscopically classified as stars were extracted from the spectroscopic data base using all data obtained up to January 4, 2005. Because the SDSS observes the high-latitude sky and has a bright limit of about 14, most of the stars observed lie in the Galactic halo and thick disk. In particular, the F subdwarfs, sixteen of which are observed for every plate to act as photometric standards, lie in the halo. A small fraction of stars has been observed spectroscopically more than once, either to provide quality checks for the data or occasionally by chance (this is especially true for the spectrophotometric standard stars). The data for stars observed more than once, 10 647 in all, were then identified.

The $u - g$ vs. $g - r$ color–color diagram for these stars is shown in the left panel of Fig. 1. The stars cover essentially the full range of stellar colors observed by SDSS (see Finlator et al. 2000). The large number of stars in the F subdwarf region occurs because of the use of these objects as spectrophotometric standards; they are the only stars for which SDSS observes a representative sample.

For a given multiply-observed star, we have a set of observations of $V \pm \epsilon$, the heliocentric radial velocity and its uncertainty. The right panel of Fig. 1 shows the mean ϵ versus color for the sample of stars. As expected, the uncertainty of the radial velocities is color-dependent, with large values for $u - g < 0.5$. This occurs because many of the blue stars are

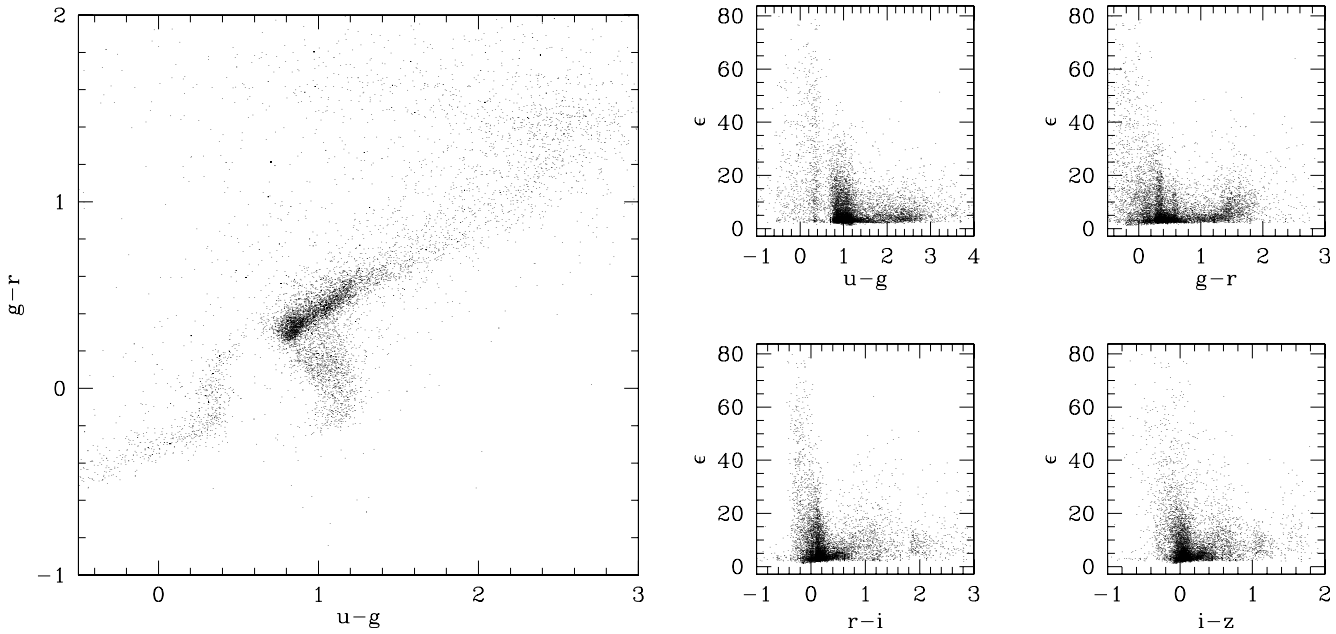

Fig. 1. (*Left panel*) Color–color diagram of the 10 647 stars with multiple SDSS spectral observations. The colors are uncorrected for interstellar extinction. (*Right panel*) Mean radial velocity uncertainty (km s^{-1}) versus color.

white dwarfs, whose very broad lines preclude the measurement of the radial velocity to accuracies of 10 km s^{-1}, which are typical for the observations of main sequence stars (see below). Note also that the 45-min exposure time for the spectroscopic observations will lead to broadening of the spectral lines of stars with rapidly-varying velocities, and that additional uncertainties can be introduced by the assumption of a single radial velocity for all spectral lines.

4. Velocity accuracy and incidence of binary stars

First, we check the quoted accuracies ϵ of the radial velocities by comparing them with the velocity dispersion σ for multiply-observed stars. In most of these cases, the star has been observed only twice, but 182 stars in the SDSS "Southern Survey" – a region of sky ±1.25° in declination along the celestial equator (J2000) between right ascensions 20^h to 04^h – have been observed often enough (six or more times) that a reasonable estimate can be made of the dispersion σ in radial velocity. The resulting values of σ were compared with ϵ for each star, and the ratio σ/ϵ computed (upper left panel of Fig. 2). This distribution is expected to have a tail to high values because of the presence of spectroscopic binaries in the sample, but if the fraction of binaries is small (see below) the median value of σ/ϵ will be little affected by their presence (upper right panel of Fig. 2). We find the median to be 1.5, and it does not depend on the available number of observations for each star – i.e. the same median is found for stars with six or more observations, seven or more, and so on. Thus the data suggest that the fitted velocity uncertainties ϵ may underestimate the true errors σ by a factor of about 1.5.

Let us now turn to binary detection. Since the number of observations of each star is small, we search for radial velocity variations by determining the maximum excursion of the

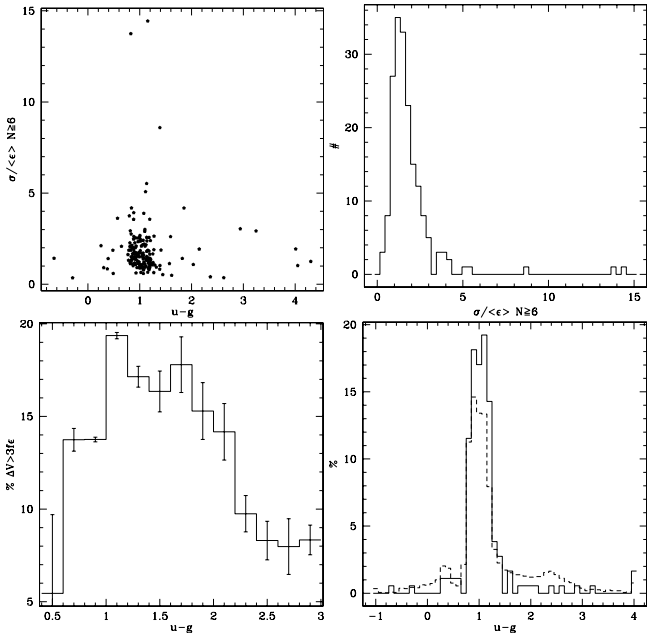

Fig. 2. (*Upper left panel*) Ratio of the standard deviation of the velocity of stars observed six times or more reckoned in mean quoted velocity uncertainty versus color. (*Upper right panel*) Distribution of that ratio. (*Lower left panel*) Percentage of stars with $u - g > 0.5$ and significant velocity excursions (see text). (*Lower right panel*) Color distribution of the 10 674 stars (dashed line) and those with significant velocity excursions (solid line).

observed velocities, $\Delta V = V_{\max} - V_{\min}$, and asking if its value is consistent with the quoted uncertainties. If $(p_1, \ldots, p_n)$ are n values drawn from a $N(m, \sigma)$ distribution, then

$$\max(p_1, \ldots, p_n) - \min(p_1, \ldots, p_n) \sim N(0, f(n)\sigma)$$

Table 1. Number of stars ($N_{\rm obj}$) versus the number of repeated observations ($N_{\rm obs}$). f is the multiplier for the standard deviation when the maximum excursion of the data is measured (see text) and grows with $N_{\rm obs}$.

$N_{\rm obs}$	$N_{\rm obj}$	f	$N_{\rm obs}$	$N_{\rm obj}$	f	$N_{\rm obs}$	$N_{\rm obj}$	f
2	9108	1.41	6	45	2.68	10	24	3.17
3	938	1.91	7	35	2.83	11	7	3.27
4	287	2.24	8	34	2.96	12	9	3.35
5	132	2.48	9	27	3.08	13	1	3.42

where f depends on the number of observations, e.g. $f = \sqrt{2}$ for two observations. We determined f for larger n using Monte-Carlo simulations. For a given star, the individual values of ϵ are almost always very similar, so we make the simplifying assumption of a constant value of ϵ (just the average) for all the observations of that star. We then conclude that a given star shows significant velocity variations if $\Delta V > 3f\epsilon$. For the 10 647 stars with multiple observations, Table 1 lists the distribution of the number of observations and the corresponding values of f determined from Monte-Carlo simulations.

The lower left panel of Fig. 2 shows the percentage of stars for which $\Delta V > 3f\epsilon$ as a function of color. The mean percentage (for $0.7 \leq u-g \leq 2.2$) is about 15% but it does not seem to be constant with color. After a steep raise at $u-g \sim 1$, it decreases at a nearly constant rate up to $u-g \sim 2.7$. It is likely that such a decrease is related to the capacity of the method to detect binaries rather than to a genuine feature of the binary distribution. Still, this mean percentage is about 50 times higher than the rate expected if the radial velocities were constant and the velocity errors Gaussian. The quantity $\Delta V/1.5f\epsilon$ was computed for the entire sample of 10 647 stars. The fraction of stars for which this quantity is greater than 3 drops to 6.5%. Figure 3 shows the histogram of velocity offsets. Almost all of the data (>90%) are consistent with Gaussian velocity errors.

Since we have only a few (mostly only two) observations of each star, and these are randomly distributed in terms of the orbital periods, we do not expect to be able to identify every binary star even for those with velocity amplitudes several times the SDSS velocity uncertainties. In order to estimate the detection rate, synthetic observations with same time distribution and uncertainty as the original observations are generated using the compilation of orbital elements for 2405 spectroscopic binary stars from S_{B^9}[1] (Pourbaix et al. 2004b). Each one of the 10 647 stars is tested against every single orbit. The maximum velocity excursions ΔV is derived and so is the percentage of simulated observations with $\Delta V > 3f\sigma$, where σ is defined to be 1.5 times the mean quoted velocity error ϵ. This simulation shows that only 39% of these synthetic binaries would be identified by the existing SDSS observations. The percentage reaches 57% for stars observed six times or more. Combining this result with the 6.5% of 3σ binaries within the sample of stars observed more than once by SDSS which show detectable velocity variations, one ends up with 16.7% of stars in the halo which are spectroscopic binaries, very consistent with the value of 18% ± 4% found by Carney et al. (2003). Owing to the effect of the rotation on the precision of the radial velocities and, therefore, on the significance of the largest radial velocity difference, our inferred percentage of binaries is a lower bound.

[1] http://sb9.astro.ulb.ac.be

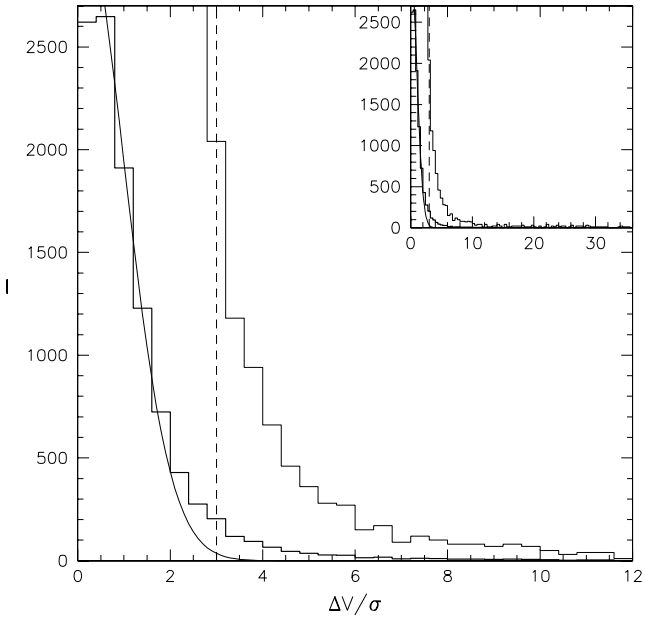

Fig. 3. Distribution of errors for multiply- observed stars, showing the number of stars versus the normalized velocity excursion, $\Delta V/\sigma$ (see text). The inset shows the full range of this quantity. The distribution is plotted twice: the light histogram shows the distribution with the vertical axis magnified by 10. The vertical dotted line shows the 3σ criterion used to identify possible binary stars (see text). A Gaussian with dispersion 1 and total number of objects equal to that in the sample is compared (light curve) with the observed distribution (histogram, heavy line).

5. Spectroscopic orbits

Nineteen multiply-observed stars have enough observations and a large enough velocity excursion with respect to the errors that an orbit can in principle be found (a minimum of six observations is required to define an orbit, but these must be accurately measured and well distributed with phase), as shown by the simulations described above. Since the maximum number of observations per object available from our observations is thirteen and these are not necessarily well distributed, a robust orbit determination is unlikely and the orbits calculated in this section must be regarded as preliminary. The nineteen objects are listed in Table 2 along with their SDSS *ugriz* magnitudes and the spectral type assigned by the velocity fitting program. Upon examination of the data, four of these were discarded: SDSS J030953.46+002747.5, J031505.31+002120.4, J031559.14+002803.2, and J032937.49+000443.7. For example, the orbit fit to SDSS J030953.46+002747.5 is very eccentric ($e = 0.978$), which would make it an outlier in the $e - \log P$ diagram (Pourbaix et al. 2004a), and discarding the most discrepant observation leaves only five points, too few for an orbital fit. The situation for the three other stars is essentially the same. These four stars are among the faintest of the sample. Even when the most discrepant velocity is removed,

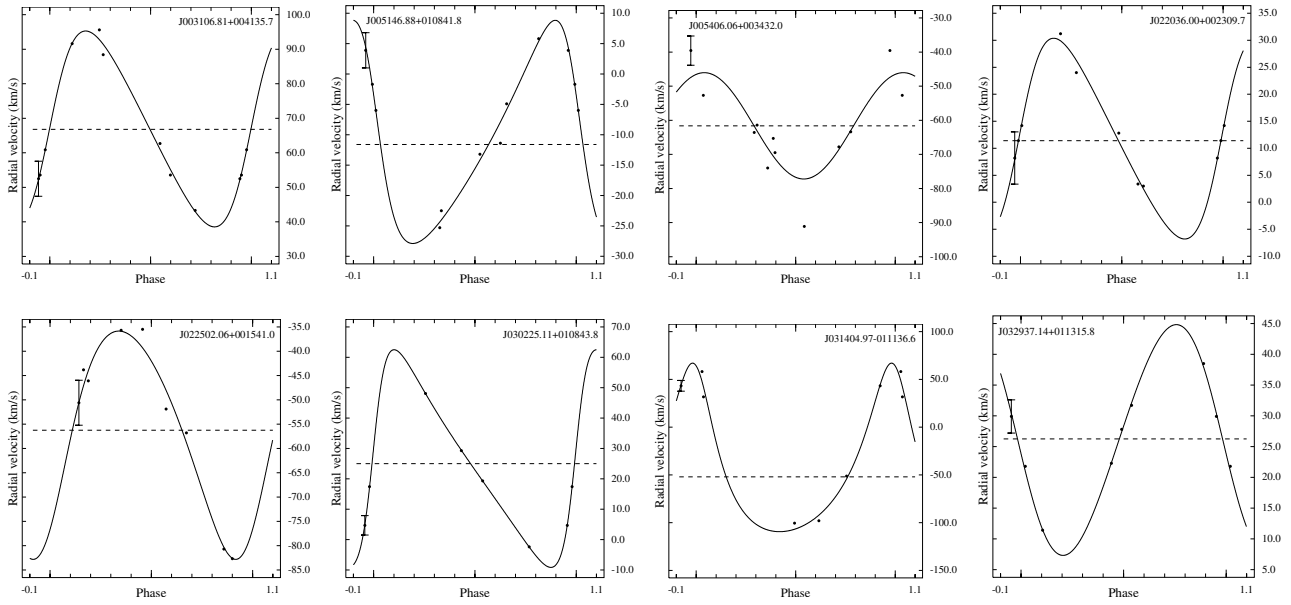

Fig. 4. Plots of the orbits given in Table 3. The dashed line shows the systemic velocity.

Table 2. Stars for which there are enough observations to potentially derive a spectroscopic orbit. N is the number of observations and $\langle\epsilon\rangle$ the mean of the quoted radial velocity uncertainties (km s^{-1}). The remaining columns list the *ugriz* magnitudes and the derived spectral type Sp.

Name (SDSS J.)	N	$\langle\epsilon\rangle$	u	g	r	i	z	Sp
003106.81+004135.7	10	3.2	18.93	17.79	17.26	17.04	16.91	F9
003546.95+001303.5	9	3.1	17.49	16.41	15.93	15.77	15.71	G2
005146.88+010841.8	9	2.9	17.75	16.56	16.07	15.89	15.78	F9
005406.06+003432.0	10	4.3	18.09	17.28	16.99	16.88	16.85	F2
022036.00+002309.7	8	3.1	17.54	16.44	15.99	15.84	15.79	F9
022216.99+000611.9	9	2.1	16.76	15.92	15.60	15.50	15.49	F2
022426.98+004236.4	9	2.8	16.97	15.90	15.48	15.35	15.30	G2
022502.06+001541.0	9	4.4	18.69	17.89	17.51	17.39	17.33	F2
022555.65+010850.3	9	2.5	17.03	16.20	15.92	15.82	15.77	F2
030225.11+010843.8	6	3.2	17.95	16.84	16.35	16.15	16.07	G2
030953.46+002747.5	6	4.1	20.65	18.80	17.78	17.70	16.99	K5
031404.97-011136.6	6	5.7	20.78	19.95	19.12	17.80	17.01	M3
031505.31+002120.4	7	14.4	25.51	22.27	20.44	19.18	18.33	M2
031540.79+002830.0	6	3.2	19.60	18.21	17.46	17.15	16.92	F9
031559.14+002803.2	7	9.1	23.11	22.54	20.97	18.87	17.77	M4
032937.14+011315.8	7	2.7	17.54	16.44	15.95	15.74	15.62	F5
032937.49+000443.7	6	5.7	19.40	18.52	18.10	17.95	17.83	F2
033209.68+005658.1	8	3.1	18.36	17.36	16.86	16.67	16.57	F5
034137.67+011027.6	6	3.8	18.78	17.63	17.17	16.98	16.87	F5

the remaining data still exhibit a significant velocity excursion, supporting their identification as binary stars. For seven other stars, either the amplitude or the period is poorly constrained, and these preliminary solutions are not included.

The orbits for the remaining eight stars are reasonably robust and are given in Fig. 4 and Table 3. This table lists the name of the object, its systemic velocity V_0, the eccentricity e, the argument of the periastron ω, the projected radial velocity amplitude K, the period P, and one epoch of periastron passage T_0. Also listed are the projected semi-major axis of the absolute orbit of the primary $a_1 \sin i$, the mass function $f(M)$ (Binnendijk 1960), the value of χ^2 and the goodness of fit F2 (Kovalevsky & Seidelmann 2004)

$$F2 = \sqrt{\frac{9\nu}{2}}\left(\sqrt[3]{\frac{\chi^2}{\nu}} + \frac{2}{9\nu} - 1\right)$$

where ν is the number of degrees of freedom, i.e. the number of observations minus 6. $F2$ follows a $N(0, 1)$-distribution, and is <3 for all the stars (though it is undefined when the number of observations equals the number of orbital parameters). Based on the algorithm by Eyer & Bartholdi (1999), the Nyquist frequency is one per day, and none of the derived periods is below that limit. The eccentricities of the eight orbits are consistent with those of similar systems (spectral type, orbital period) found in S_{B^9}.

SDSS J031404.97-011136.6 has the largest signal to noise ratio of the sample and also exhibits the largest mass function $f(M)$. The colors, $r - i = 1.32$ and $i - z = 0.78$, correspond to an M3 star (Hawley et al. 2002) and the fits to all 7 spectra also yield M3. Examination of the spectra (one of which is shown in Fig. 5) shows that this is a dM/WD pair, consistent with the white dwarf being the more massive of the pair. However, the mass function, 1.9 ± 0.4 solar masses is about 3σ different from typical values found for these objects.

In all, we found 675 stars with velocity excursions large enough that they are likely to be spectroscopic binaries. This list is given in Table 4 (available only in electronic form at CDS). It includes 13 M dwarf-white dwarf (dM/WD) pairs and 7 cataclysmic variables (CVs), easily identified by eye examination of the spectra. These latter are described by Szkody et al. (2002, 2003a,b, 2004, 2005), but one observation of note is not included in those papers. The second observed spectrum of SDSS J090628.25+052656.9, on MJD 2 452 674, is presented by Szkody et al. (2005) and shows both red and blue stellar components and hydrogen Balmer line emission. A spectrum obtained a month earlier, however (MJD 2 452 649) catches the

Table 3. Orbital elements and their uncertainty. V_0 and K are in km s^{-1}, ω in degrees, P in days, epoch T_0 is in days + 2 400 000, $a_1 \sin i$ in 10^6 km and $f(M)$ in solar masses.

Name	V_0	e	ω	K	P	T_0	$a_1 \sin i$	$f(M)$	χ^2
	σ_{V_0}	σ_e	σ_ω	σ_K	σ_P	σ_{T_0}	$\sigma_{a_1 \sin i}$	$\sigma_{f(M)}$	$F2$
003106.81+004135.7	66.80	0.222	271	28.4	14.18	51793.7	5.4	0.0312	2.26
	0.77	0.057	17	0.7	0.98	0.55	0.4	0.0082	–0.060
005146.88+010841.8	–11.60	0.343	71	18.4	5.98	51814.2	1.4	0.0032	1.73
	0.62	0.045	24	1.9	0.58	0.24	0.2	0.0015	–0.34
005406.06+003432.0	–61.6	0 (fixed)	345	15.58	15.9	51806.3	3.40	0.0062	14.63
	1.2	–	–	0.62	1.1	0.54	0.27	0.0017	2.53
022036.00+002309.7	11.4	0.234	275	18.6	8.85	51820.5	2.2	0.0054	0.84
	1.1	0.071	27	2.4	0.35	0.54	0.3	0.0023	–0.42
022502.06+001541.0	-56.2	0.179	222	23.48	3.57	51819.3	1.136	0.00458	2.64
	0.6	0.046	12	0.8	0.11	0.13	0.054	0.00071	0.12
030225.11+010843.8	24.99	0.448	276.0	35.8	117.3	51822.2	51.7	0.401	6.1e-4
	0.87	0.034	5.6	2.1	2.3	0.95	3.3	0.078	–
031404.97-011136.6	–52.0	0.361	14.8	88	32.8	51873.5	37.0	1.90	7.82
	2.5	0.034	8.8	4	1.3	0.36	2.3	0.38	–
032937.14+011315.8	26.26	0 (fixed)	97	18.7	21.77	51869	5.60	0.0148	0.19
	0.78	–	–	2.1	0.54	2.3	0.64	0.0051	–0.43

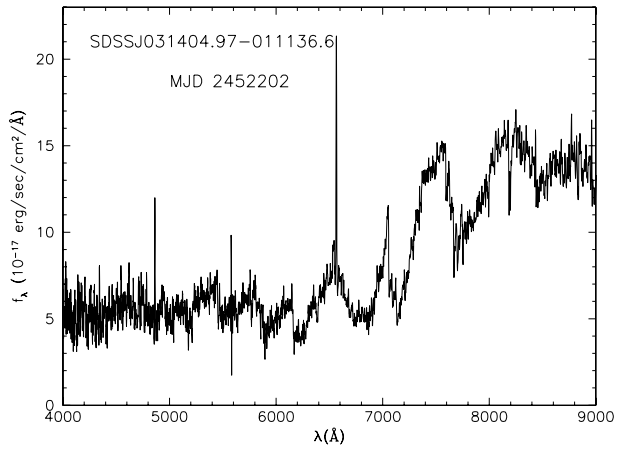

Fig. 5. Spectrum of SDSS J031404.97-011136.6. This star is an example of a white dwarf-M dwarf pair, as shown by the blue continuum (well in excess of that expected from a dM3 star) and the strong Hα emission, which may be due to irradiation of the dM secondary by the white dwarf.

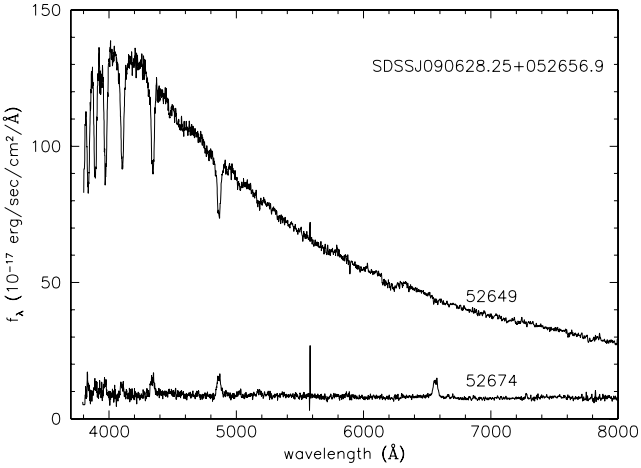

Fig. 6. Spectra of the CV SDSS J090628.25+052656.9 labelled by MJD (–2 400 000) of observation. The system is observed in both its low and high states. In the high state, rotationally broadened Balmer absorption lines are seen, and Hα is filled in by emission.

star in its high state. These spectra are shown in Fig. 6 and are available at the SDSS web site (they can be located using the information in Table 4). Szkody et al. (2005) note that this star is a likely dwarf nova, and the outburst spectrum shown in Fig. 6 lends support to this classification. Further, the four observations of this object (Fig. 6 and Szkody et al. 2005) find it in outburst twice – thus the outbursts likely repeat on a fairly short timescale.

Finally, none of the 35 carbon stars with multiple observations shows significant radial velocity deviations.

6. Conclusions

We examine some 10 000 stars for which multiple SDSS spectra have been obtained. The dispersion of the measured velocities is found to be about 1.5 times the quoted uncertainty of the radial velocity fits for stars of all observed colors (spectral types) and magnitudes. A group of objects with large velocity excursions is identified and the percentage of such stars (6%) shown to be consistent with the expected fraction of binary stars.

We identify 675 possible new binary stars. Most of these, like most of the observed stars, are F subdwarfs, but the list includes 13 dM/WD pairs and 7 CVs. One of these, SDSS J090628.25+052656.9, is observed in both its low and high states. The identification of these 675 stars as binaries is very preliminary, being based on a very small number of observations. The number of false positive identifications is estimated to be about 40 from simulations. However, since these stars will not be further observed by SDSS, they are presented here as candidates for possible future study.

Eight of the stars have enough observations (6–13) and show large enough velocity excursions with respect to the uncertainties that the fitted orbit is reasonably robust. These orbits and the corresponding radial velocities are available on S_{B^9}.

Acknowledgements. We thank the referee for many helpful comments which significantly improved the paper. Partial support for the computer systems required to process and store the data was provided by NASA via grant NAG5-6734 and by Princeton University. D.P. thanks the American Astronomical Society for the award of a Chrétien International Research Grant. We also thank Princeton University for generous support. This research made use of the IDL Astronomy User's Library at Goddard.

Funding for the creation and distribution of the SDSS Archive has been provided by the Alfred P. Sloan Foundation, the Participating Institutions, the National Aeronautics and Space Administration, the National Science Foundation, the US Department of Energy, the Japanese Monbukagakusho, and the Max Planck Society. The SDSS Web site is `http://www.sdss.org/`. The SDSS is managed by the Astrophysical Research Consortium (ARC) for the Participating Institutions. The Participating Institutions are The University of Chicago, Fermilab, the Institute for Advanced Study, the Japan Participation Group, The Johns Hopkins University, the Korean Scientist Group, Los Alamos National Laboratory, the Max-Planck-Institute for Astronomy (MPIA), the Max-Planck-Institute for Astrophysics (MPA), New Mexico State University, University of Pittsburgh, University of Portsmouth, Princeton University, the United States Naval Observatory, and the University of Washington.

References

Abazajian, K., Adelman-McCarthy, J. K., Agüeros, M. A., et al. 2003, AJ, 126, 2081
Abazajian, K., Adelman-McCarthy, J. K., Agüeros, M. A., et al. 2004, AJ, 108, 502
Abazajian, K., Adelman-McCarthy, J. K., Agüeros, M. A., et al. 2005, AJ, 129, 1755
Beers, T. C., Allende Prieto, C., Wilhelm, R., Yanny, B., & Newberg, H. 2004, PASA, 21, 207
Binnendijk, L. 1960, Properties of Double Stars (University of Pennsylvania Press)
Blanton, M. R., Lin, H., Lupton, R. H., et al. 2003, AJ, 125, 2276
Carney, B. W., Latham, D. W., Stefanik, R. P., Laird, J. B., & Morse, J. A. 2003, AJ, 125, 293
Eyer, L., & Bartholdi, P. 1999, A&AS, 135, 1
Finlator, K., Ivezić, Ž., Fan, X., et al. 2000, AJ, 120, 2615
Fukugita, M., Ichikawa, T., Gunn, J. E., et al. 1996, AJ, 111, 1748
Gunn, J. E., Carr, M., Rockosi, C., et al. 1998, AJ, 116, 3040
Hawley, S. L., Covey, K. R., Knapp, G. R., et al. 2002, AJ, 123, 3409
Heyer, M. H., & Schloerb, F. P. 1997, ApJ, 475, 173
Hogg, D. W., Finkbeiner, D. P., Schlegel, D. J., & Gunn, J. E. 2001, AJ, 122, 2129
Ivezić, Ž., Lupton, R. H., Schlegel, D., et al. 2004, Astron. Nachr., 325, 583
Kovalevsky, J., & Seidelmann, P. K. 2004, Fundamentals of Astrometry (Cambridge University Press)
Lupton, R. H., Gunn, J. E., Ivezić, Ž., et al. 2001, in ASP Conf. Ser. 238, ed. F. R. Harnden, F. A. Primini, & H. E. Payne, 269
Lupton, R. H., Ivezić, Ž., Gunn, J. E., et al. 2003, Proc. SPIE, 4836, 350
Moultaka, J., Ilovaisky, S. A., Prugniel, P., & Soubiran, C. 2004, PASP, 116, 693
Oke, J. B., & Gunn, J. E. 1983, ApJ, 266, 713
Pier, J. R., Munn, J. A., Hindsley, R. B., et al. 2003, ApJ, 125, 1559
Pourbaix, D., Ivezić, Ž., Knapp, G. R., Gunn, J. E., & Lupton, R. H. 2004a, A&A, 423, 755
Pourbaix, D., Tokovinin, A. A., Batten, A. H., et al. 2004b, A&A, 424, 727
Prugniel, P., & Soubiran, C. 2001, A&A, 369, 1048
Raymond, S. N., Szkody, P., Hawley, S. L., et al. 2003, AJ, 125, 2621
Smith, J. A., Tucker, D. L., Kent, S., et al. 2002, AJ, 123, 2121
Smolčić, V., Ivezić, Ž., Knapp, G. R., et al. 2004, ApJ, 615, L141
Szkody, P., Anderson, S. F., Agüeros, M., et al. 2002, AJ, 123, 430
Szkody, P., Anderson, S. F., Schmidt, G., et al. 2003a, ApJ, 583, 902
Szkody, P., Fraser, O., Silvestri, N., et al. 2003b, AJ, 126, 1499
Szkody, P., Henden, A., Fraser, O., et al. 2004, AJ, 128, 1882
Szkody, P., Henden, A., Fraser, O., et al. 2005, AJ, 2386
Uomoto, A., Smee, S., Rockosi, C., et al. 1999, BAAS, 31, 1501
York, D. G., Adelman, J., Anderson, J. E., et al. 2000, AJ, 120, 1579